RSC Advances

ROYAL SOCIETY OF CHEMISTRY

www.rsc.org/advances

A highly selective and sensitive electrochemical determination of melamine based on succinic acid functionalized copper oxide nanostructures

Razium Ali Soomro[a,b], Keith Richard Hallam[a], Zafar Hussain Ibupoto[b]*, Aneela Tahira[b], Sana Jawaid[c], Syed Tufail Hussain Sherazi[c], Sirajjuddin[c], Magnus Willander[d]

[a] Interface Analysis Centre, School of Physics, University of Bristol, Bristol, BS8 1TL, UK

[b] Dr M.A. Kazi Institute of Chemistry, University of Sindh, Jamshoro, 76080, Pakistan

[c] National Centre of Excellence in Analytical Chemistry, University of Sindh, Jamshoro, 76080, Pakistan

[d] Department of Science and Technology, Campus Norrkoping, Linkoping University, SE-60174 Norrkoping, Sweden

Abstract

This study presents the development of highly selective and sensitive electrochemical sensor for the determination of melamine from aqueous environments. The sensor system is based on functionalised marigold-like CuO nanostructures fabricated using controlled hydrothermal process, where the utilised succinic acid is considered to play a dual role of functionalising and growth controlling agent (modifier). The fabricated nanostructures exhibit sharp and well-ordered structural features with dimension (thickness) in range of 10-50 nm. The sensor system exhibits firm linearity within the concentration range of 0.1×10^{-9} to 5.6×10^{-9}M and demonstrates excellent limit of detection up to 0.1×10^{-10} M. The extreme selectivity and sensing capability of the developed sensor is attributed to the synergy of selective interaction between succinic acid and melamine moieties, added by the high surface area of marigold-like CuO nanostructures. In addition to this, the developed sensor was also utilised for the determination of melamine from real milk samples collected from different regions of Hyderabad, Pakistan. The obtained excellent recoveries proved the feasibility of the sensor for real life applications. The sensor system offers an operative measure for detecting extremely low melamine content with high selectivity in food contents.

Keywords: Succinic acid, CuO nanostructures, melamine, milk, sensor

*Corresponding author. Tel.: + 92 336 3051253; Fax: + 92 22 9213431

E-mail address: zaffar_ibupoto@yahoo.com (Zafar Hussain Ibupoto)

1. INTRODUCTION

The metal oxide nanostructures based on their unique characteristic have demonstrated potential applications in the area of electrochemical sensors. The versatility of such nanostructures ranges from the sensitive determination of toxins to the various bio-molecules in complex matrix system[1]. From the diverse range of metal oxides available, copper oxide (CuO) in particular has drawn significant research attention because of its superior electrochemical characteristics compared to its other oxide based competitors[2]. Besides this, CuO is also known to possess excellent surface activity, adsorption capability and electronic properties[3]. Over the past decade, a new dimension has emerged in the area of metal oxide associated electrochemical sensors based on the fact that the structural morphology of such nanostructures may significantly contribute towards the sensitivity and selectivity of the developed sensor[4, 5]. In this regard, various morphologies of CuO have been reported as electrode material for the non-enzymatic glucose sensing[6]. Although, the reported sensors had rapid response times, high reproducibility and stability, but the sensitivities of such sensor were found highly dependent on the nanostructures morphology[7-9]. Cao, Monnell et al. (2007)[10] demonstrated the capability of CuO nanostructures (microsphere, doughnut-like and multi-layered microsphere) for arsenic (III) removal from aqueous system and very recently, Senthilkumar, Kim et al. (2015)[11] demonstrated the excellent specific capacitance associated with nanopaltes of CuO compared to other morphologies like bud and flower shaped nanostructures. The aforementioned reports clearly indicate the strong dependence of electrochemical behaviour on the structural features of CuO nanostructures. Thus, fabricating highly attractive and morphologically uniform nanostructures with high structural reproducibility is an important issue when it comes to the production of highly reliable electrochemical sensors. In this context, application of modifiers can result in highly reproducible and controlled metal oxide nanostructures. The usage of such molecules not only ensure development of robust and stable sensor system, but also enables directional growth leading to new and unique structural architectures with much enhanced electrochemical properties compared to their modifier free partners[12].

Despite the extensive applications of CuO in numerous areas, the capability of copper oxide as an electrode material for the electrochemical sensing of food toxins is very less explored. The constant global upsurge in food demand has resulted in overall increase in food adulteration to gain greater financial benefits. Melamine in this context is one of the most common adulterant found in protein rich deities such as eggs, biscuits, milk, candy and

coffee. Melamine is also known to produce insoluble complex with cyanuric acid which results in crystallization and subsequent tissue damage such as urolithiasis and bladder cancer[13]. The extensive usage of melamine has been observed in the developing countries like Algeria, Pakistan, China and India where it is primarily used for milk adulteration[14]. The conventional techniques like gas chromatography (GC)[15], high pressure liquid chromatography (HPLC)[16], surface enhanced raman spectroscopy [17] and capillary zone electrophoresis/ mass spectrum (CE/MS) [18] are highly sensitive towards the determination of melamine. However, the tedious sample preparation steps, high commercial cost and lengthy protocols associated with these techniques restricts their application in a wider scope. In contrast, the electrochemical approach is considered much suitable based on pros like fast analysis time, sensitive nature and simplicity. Besides this, electrochemical approach also enables miniaturisation of the device which promises the development of convenient, portable yet inexpensive sensor systems. At present most of the developed electrochemical sensors utilise indirect approach for the determination of melamine because of the associated electro-inactivity [19]. The most common approach involves the usage of redox mediators or probes to detect the presence of melamine in complex matrix. Liao, Chen et al. (2001)[20] reported the electrochemical determination of melamine using disposal screen printed carbon electrodes with uric acid as detecting probe. Similarly, Liu, Deng et al. (2011) [13] and Akter, Shaikh et al. (2013) [21]demonstrated the usage of hexacyno ferrate as a redox probe for melamine sensing. Improvements in the electrochemical assay have been achieved via usage of metal oxides as electrode modifying material. Recently, Rovina and Siddiquee (2016) [22] reported the application of ionic liquid/zinc oxide nanoparticles/chitosan/gold electrode for the determination of melamine in presence of methylene blue (MB) as indicator. The enhanced signal response was attributed to the extremely high surface area of ZnO nanoparticles and facilitation of redox process due to favourable electrostatic charges associated with the used ionic liquid. However, like most of the analytical assays for melamine, the signal (current) depends on the employed redox indicator which results in poor sensitivity and selectivity of developed sensor system.

In this paper, we present a novel approach towards the determination of melamine by utilising succinic acid modified CuO nanostructures as electrode material in the absence of any redox indicator. The extreme surface characteristics of CuO combined with electroactive complex formed as a consequence of interaction between the active moieties (carbonyl) of functionalisation agent (succinic acid) and melamine enables development of highly selective

and sensitive electrochemical melamine sensor. The robust nature of the developed sensor system was evaluated by observing its capability to determine melamine from dairy milk and urine samples collected from the local vendors and district children hospital of Hyderabad region, Pakistan respectively.

2 Experimental

2.1 Materials

All the chemical utilized in this study were analytical grade: copper chloride ($CuCl_2 \cdot 2H_2O$), succinic acid ($C_4H_6O_4$), melamine ($C_3H_6N_6$), 38% ammonia solution (NH_3), nafion ($C_7HF_{13}O_5S.C_2F_4$) and sodium hydroxide (NaOH) were purchased from Sigma Aldrich. 1.0 % nafion solution in isopropanol solvent (C_3H_8O) (Merck) was utilised as electroactive polymer. The utilised nano-molar concentration of melamine was prepared by carrying successive dilution of standard 1 µM (1.26 µg/ 10ml) melamine solution to obtain 5.6×10^{-9} M solution. This solution was further diluted in series to produce 0.1 $\times10^{-9}$ M solution with successive step of 9.2 ml in fixed 0.8 ml of de-ionised water.

while all other solutions were prepared using milli-Q water.

2.2 Synthesis of functionalised CuO nanostructures

The hydrothermal strategy was utilised for the synthesis of CuO nanostructures. In a typical experiment, $CuCl_2 \cdot 2H_2O$ (1.5 g) was sufficiently vortexed with succinic acid (2 g) in 95 ml of di-ionised water. The mixture was further introduced 5 ml of 38% (NH_3) solution as a precipitating agent and the container was tightly sealed using an aluminium foil to prevent any solvent spillage. The mixture was then hydrothermally treated in a pre-heated electrical oven at 85 ˚C for about 8 hr. The grown nanostructures were then separated from the container using simple filtration process and washed with de-ionized water to remove any surface bound impurities. Herein, the employed succinic acid plays a dual role of modifier as well as functionalising agent for copper oxide nanostructures. The choice of using succinic acid was based on the fact that it contains double carbonyl moieties which are known to have strong interaction with melamine molecules via hydrogen bonding and electrostatic forces leading to an electroactive complex as further described in section (3.2).

2.3 Material characterisation and electrochemical measurement

Field emission gun scanning electron microscopy (FEG-SEM) (Zeiss SIGMA) and x-ray diffraction (XRD) (Bruker D-8) and x-ray photoelectron spectroscopy (XPS) (Scienta ESCA200) were utilised for morphological, structural and compositional characterisation respectively. Electrochemical testing was carried on a Bipotentiostate model 760E (CH Instruments USA).

2.4 Preparation of modified glassy carbon electrode (GCE) and their electrochemical evaluation

The modification of glassy carbon electrode with succinic acid functionalised CuO nanostructures was carried using simple drop cast methodology. Earlier to modification, the GCE was thoroughly washed with di-ionised water and polished with 1 μm and 0.05 μm alumina slurry respectively to obtain a mirror shiny surface. The clean electrode was then subjected to ultrasonic bath of de-ionised water and ethanol to assure complete removal of any surface bound impurities. The polished GCE was then allowed to dry under ambient air condition followed by drop casting, 5 μL suspension (1 mg/ml in methanol) of functionalised CuO nanostructures over the surface of GCE. To ensure proper adherence of the functionalised nanostructures on the surface of GCE, a layer of nafion (5 μL) was deposited and dried under nitrogenous atmosphere. The modified GCE was further utilised as a working electrode in a three electrode cell assemble of Ag/AgCl and Pt wire taken as a reference and counter electrode respectively. The working electrode is denoted as GCE/CuO-NSs/nafion throughout the entire manuscript.

3 Results and discussion

3.1 The morphological characteristics of CuO nanostructures

The synthesised CuO nanostructures were grown using succinic acid employed both as modifier as well as functionalising agent. The ability of succinic acid to direct the growth of CuO nanostructures is clearly visible from the captured FEG-SEM images at various magnifications shown in Figure 1.

Figure 1

The as-synthesised nanostructures clearly depict sharp and regular morphological features with similarity to marigold flower. The average thickness of formed petals was estimated to be in range of 10-50 nm. The dense distribution of the obtained nanostructures

with high order in formation may be attributed to the strong growth controlling and directing capability of succinic acid. The contribution of the modifier towards growth of nanostructures was further confirmed by synthesising CuO in similar experimental conditions without the usage of suggested modifier. As expected, the synthesised structures were enormous in size, with no any regularity and proper structural features as seen in Figure S1. The high modifying efficiency of succinic acid may be attributed to the strong polarization of the associated carbonyl moieties, resulting in strong interaction for Cu^{+2} nuclei during the hydrothermal grown process[23]. The general growth pattern can be visualised by the schematic diagram presented in Figure S2. Initially the interaction of Cu^{+2} ions and succinic acid enables formation of nuclei with loosely bonded succinic acid. These dangling di-carboxylic molecules then further allow spontaneous aggregation favoured by constant thermal treatment. With the passage of time, these nuclei are directed by succinic acid under an orderly fashion to grow and form marigold-like structure. The efficiency of succinic acid may be attributed to its di-carboxylic nature which unlike multi-functional modifier enables succinic acid to demonstrate identical modifying capability for both moieties leading to highly ordered and well-structured nanomaterial.

The phase composition of synthesised marigold-like CuO nanostructures was determined using XRD analysis. The generated pattern (Figure 2) consists of intense peaks indexed to monoclinic phase of CuO as referenced against JCPDS Card No. 45-0937. The purity of as-synthesised nanostructures in terms of surface composition was assessed via XPS analysis. The wide scale spectrum shown in Figure 3 integrates major peaks inferred to C1s, O1s, Cu $2p_{3/2}$, Cu 3s and Cu 3p respectively. The full scan spectrum was further regionalised to provide information regarding functionalised moieties. The deconvoluted C1s scan presented in Figure 3(a) contains peaks around 284.4 and 288.9 eV. These may be attributed to carbon atom attached to carbonyl group and within the carbonyl moiety. The regional scan for O1s (Figure 3(b))contains peaks around 529.5 attributed to O^{-2} of CuO, 531.1 related to surface adsorbed oxygen whereas the peak around 532.6 eV is an overlap of binding energy for carbonyl and hydroxyl oxygen of succinic acid as indicated by Taheri, P., et al. (2011)[24]. Although well-resolved and intense peaks for the specific binding energies of succinic acid were not observed during the regional scan, however their presence clearly indicated the surface functionalisation of synthesised CuO nanostructures with succinic acid. Figure 3(c) represents the regional scan for Cu2p containing major peak at 933.6 eV related to $Cu2p_{3/2}$ binding energy. In addition peaks around 121.2 and 77 eV are attributed to Cu 3s and Cu 3p.

The obtained general chemical information is similar to other reports related to CuO suggesting high surface purity of as-synthesised marigold-like nanostructures[25].

Figure 2

Figure 3

3.2 The electrochemical behaviour of modified electrode

The electrochemical behaviour of the modified working electrode (GCE/CuO-NSs/nafion) was accessed in comparison to bare GCE both in the absence and presence of melamine (0.1×10^{-9} M) with 0.1 M (pH 7.5) PBS buffer. As expected, the bare GCEs exhibited no response for both cases. Whereas, well defined and intense redox peaks were produced around +0.252 and -0.252 eV for working electrode in presence of melamine as shown in Figure 4. The observed redox couples can be attributed to an electroactive complex formed at surface of modified GCE as a consequence of interaction between the carbonyl moieties of succinic acid and amines of melamine. The finding was supported by a similar study carried at pre-anodized screen printed carbon electrode[23]. Although, Liao, Chen et al. (2011), developed a selective sensor system for melamine but poor current response and sensitivity was observed due to lack of required effective surface area. Herein, the application of CuO marigold-like nanostructures offer greater surface area and enhanced conductivity to enhance the generated current response. The excellent combination of improved surface area of the unique structural features with excellent conductive of functionalised CuO enables selective and sensitive recognition of melamine molecules. The general sensing mechanism is sketched in Figure S3. To assure the observed electrochemical response is a result of interaction between succinic acid and melamine, modifier free CuO structures was employed as modifier of GCE and was evaluated in similar chemical conditions. The absence of any redox peaks (Figure 4 (b)) related to melamine indicates the significance of functional moiety (carbonyl) associated with marigold-like nanostructures.

The surface redox process was further confirmed by observing the change in measured current with the variation of scan rate in range from 0.05 to 0.11 Vs^{-1}as shown in Figure 5(a). The linear response recorded for measured current against square root of scan rate indicates reaction to be diffusion controlled as seen in the inset of Figure 5(a). The electrochemical behaviour of GCE/CuO-NSs/nafion was observed to be highly affected by the change in the pH of the system. Figure 5(b) suggests an increase in measured potential

and decrease in the generate current with increase in pH from 7-9. The reported pka value for melamine is around 8, henceforth poor response were observed near pka value, while decreasing the pH from 8 to 7.5 resulted in the optimum current response. The may be attributed to stronger electrostatic interaction between melamine and CuO surface bound succinic acid molecules. The variation in recorded responses (Figure 5(c)) was also studied against deposition volume of functionalised marigold-like nanostructures. An initial increase in the observed current was noted from 5 to 15 μL, further increment (20 μL) resulted in poor electrode performance because of the unstable current response as seen the inset of Figure 5(c). This instability might be due to the erosion of deposited material from the electrodes surface.

Figure 4

Figure 5

3.3 The analytical assessment of modified electrode

The analytical performance of the developed sensor was studied using square wave voltammetry (SWV) as a primary mode of detection. The choice of this mode was based on the reversible behaviour of the observed redox couple where SWV is considered a sensitive mode compared to its other competitors. The key parameters such as frequency, amplitude and step potential were optimised (not shown) to obtain the best possible signal for the development of highly sensitive melamine selective sensor system. The voltametric signals were recorded against concentration of melamine in range from 0.1×10^{-9} to 5.6×10^{-9} M (0.1-5.6 ppb) as shown in Figure 6. The plotted calibration along with linear regression analysis is shown in Figure 6(b). The developed sensor demonstrates excellent linearity with a correlation co-efficient (r^2) of 0.9995. The analytical sensitivity of the produced sensor was estimated to be 5.0×10^{11} μA. M^{-1}. The LOD and limit of quantification (LOQ) based on the signal-to-noise ratio (S/N) of 3, were found to be 0.1×10^{-10} and 0.4×10^{-9} M respectively. The estimated limit of detection for this assay is much smaller than observed for most recent studies concerned melamine sensing as summarised in table 1.

Figure 6

Table 1

3.4 The selectivity, reproducibility and stability of the developed sensor

The selectivity of the developed sensor was evaluated for three different categories of interferents: common co-existing molecules, cations and anions. The selected interferents were investigated with concentration 10 folds of that melamine (0.1×10^{-9} M). The corresponding SWV curves are presented in in Figure 7(a). The normalised current response along with zoomed in widow reflecting variation in measured current can be seen as inset graphs. The negligible variation in the measured current in presence of such interferents clear indicates the high selectivity of the developed sensor towards melamine. The reproducibility of the developed sensor was evaluated by measuring repetitive runs of working electrode (GCE/CuO-NSs/nafion) in 0.1×10^{-9} M melamine with 0.1 M (pH 7.5) PBS buffer. The small variation (<1.0 % RSD) in recorded current response indicates the reproducible nature of the developed sensor system (Figure 7(b)). The stability of the developed sensor was also evaluated by observing the current response of GCE/CuO-NSs/nafion in melamine (0.1×10^{-9} M) containing solution periodically during one month of electrode storage period in ambient air conditions. The negligible current variation as seen in Figure 7(c) demonstrates the high stability of the produced modified electrode system.

Figure 7

3.5 The determination of melamine in real milk and urine samples

To evaluate the performance of the sensor system for its feasibility in real world applications, the sensor was utilised for melamine determination from the milk samples collected from different regions of Hyderabad, Pakistan. The collected milk samples were pre-treated according to procedure suggested by Cao et al. (2009)[26]. The samples were analysed for the melamine using similar procedure as mentioned in section (3.3) and the obtained results are shown in table 2. Since the existing milk is supposed to be free of melamine, the prepared milk samples were spiked directly with fixed concentration of standard melamine solution. The assay enabled excellent recoveries in range from 98-99% reflecting the excellent sensing capability of the devised sensor system. To further ascertain the robustness of developed sensor system in complex real matrix environment, urine sample were analysed for presence of melamine. The urine samples were collected from local children hospital of Hyderabad and were properly diluted (50 times) with 0.1 M PBS buffer solution before analysis. The developed sensor produced excellent recoveries (table 2) for melamine in urine sample reflecting both the anti-interference potential and selectivity of the developed sensor in a complex urine based matrix.

Table 2

4.0 Conclusion

The study concentrates on the fabrication of marigold-like nanostructures using succinic acid as modifier and functionalising agent. The dual role of succinic acid enables both the formation of highly ordered nanostructures and development of highly selective electrochemical sensor for melamine in aqueous solution. The sensor utilises the interaction between carbonyl moieties of succinic acid and melamine molecules as the basis of recognition. This combined with high specific surface area offered by marigold-like CuO nanostructures is responsible for production of signal (current) which can selectively detect melamine up to 0.1×10^{-10} M. Besides this, the sensor system was found feasible for real samples analysis with excellent recoveries obtained for milk samples collected from various regions of Hyderabad, Pakistan.

Acknowledgments

We acknowledge the Higher Education Commission, Islamabad, Pakistan for funding this research under IRSIP program and the National Centre of Excellence in Analytical Chemistry, University of Sindh, Jamshoro, Pakistan for facilities during this research. The authors are highly thankful to Dr. Sidra Soomro and Dr. Gulam Raza Soomro for their co-operation in collecting children's urine samples from district hospital Qasimabad, Hyderabad Pakistan.

References

1. C. Yang, F. Xiao, J. Wang and X. Su, *Sensor Actuat B: Chem*, 2015, **207, Part A**, 177-185.
2. M. Sabbaghan, A. S. Shahvelayati and K. Madankar, *Spectrochim Acta A*, 2015, **135**, 662-668.
3. C. Yang, X. Su, F. Xiao, J. Jian and J. Wang, *Sensor Actuat B: Chem*, 2011, **158**, 299-303.
4. A. Aslani and V. Oroojpour, *Physica B*, 2011, **406**, 144-149.
5. D. Huo, Q. Li, Y. Zhang, C. Hou and Y. Lei, *Sensor Actuat B: Chem*, 2014, **199**, 410-417.
6. Z. H. Ibupoto, K. Khun, V. Beni, X. Liu and M. Willander, *Sensors*, 2013, **13**, 7926-7938.
7. L. Changli, Y. Hiroyasu, L. Yaerim, T. Hitoshi and D. Jean-Jacques, *Acs Sym Ser*, 2015, **26**, 305503.
8. Í. A. Simon, N. G. Medeiros, K. C. Garcia, R. M. D. Soares, A. T. Rosa and J. A. Silva, *Journal of the Brazilian Chemical Society*, 2015, **26**, 1710-1717.
9. R. Ahmad, N. Tripathy, Y.-B. Hahn, A. Umar, A. A. Ibrahim and S. H. Kim, *Dalton Transactions*, 2015, **44**, 12488-12492.
10. A.-m. Cao, J. D. Monnell, C. Matranga, J.-m. Wu, L.-l. Cao and D. Gao, *J. Phys. Chem C*, 2007, **111**, 18624-18628.
11. V. Senthilkumar, Y. S. Kim, S. Chandrasekaran, B. Rajagopalan, E. J. Kim and J. S. Chung, *RSC Adv*, 2015, **5**, 20545-20553.
12. Z. H. Ibupoto, A. Nafady, R. A. Soomro, Sirajuddin, S. T. Hussain Sherazi, M. I. Abro and M. Willander, *RSC Adv*, 2015, **5**, 18773-18781.
13. Y. T. Liu, J. Deng, X. L. Xiao, L. Ding, Y. L. Yuan, H. Li, X. T. Li, X. N. Yan and L. L. Wang, *Electrochim. Acta*, 2011, **56**, 4595-4602.
14. A. Kamran and S. Rizvi, in *Proceedings of the Sixth International Conference on Management Science and Engineering Management*, eds. J. Xu, M. Yasinzai and B. Lev, Springer London, 2013, vol. 185, ch. 79, pp. 909-924.
15. H. Miao, S. Fan, Y. N. Wu, L. Zhang, P. P. Zhou, J. G. Li, H. J. Chen and Y. F. Zhao, *Biomedical and environmental sciences : BES*, 2009, **22**, 87-94.
16. G. Venkatasami and J. R. Sowa Jr, *Anal. Chim. Acta*, 2010, **665**, 227-230.
17. J. Cheng and X. O. Su, *Guang pu xue yu guang pu fen xi = Guang pu*, 2011, **31**, 131-135.
18. H. A. Cook, C. W. Klampfl and W. Buchberger, *Electrophoresis*, 2005, **26**, 1576-1583.
19. Q. Cao, H. Zhao, Y. He, N. Ding and J. Wang, *Anal Chim Acta*, 2010, **675**, 24-28.

20. C.-W. Liao, Y.-R. Chen, J.-L. Chang and J.-M. Zen, *Electroanalysis*, 2011, **23**, 573-576.
21. H. Akter, A. A. Shaikh, T. R. Chowdhury, M. S. Rahman, P. K. Bakshi and A. J. S. Ahammad, *ECS Electrochemistry Letters*, 2013, **2**, B13-B15.
22. K. Rovina and S. Siddiquee, *Food Control*, 2016, **59**, 801-808.
23. C.-W. Liao, Y.-R. Chen, J.-L. Chang and J.-M. Zen, *Journal of Agricultural and Food Chemistry*, 2011, **59**, 9782-9787.
24. M. A. Dar, Q. Ahsanulhaq, Y. S. Kim, J. M. Sohn, W. B. Kim and H. S. Shin, *Appl. Surf. Sci*, 2009, **255**, 6279-6284.
25. Q. Cao, H. Zhao, L. Zeng, J. Wang, R. Wang, X. Qiu and Y. He, *Talanta*, 2009, **80**, 484-488.
1. C. Yang, F. Xiao, J. Wang and X. Su, *Sensor Actuat B: Chem*, 2015, **207, Part A**, 177-185.
2. M. Sabbaghan, A. S. Shahvelayati and K. Madankar, *Spectrochim Acta A*, 2015, **135**, 662-668.
3. C. Yang, X. Su, F. Xiao, J. Jian and J. Wang, *Sensor Actuat B: Chem*, 2011, **158**, 299-303.
4. A. Aslani and V. Oroojpour, *Physica B*, 2011, **406**, 144-149.
5. D. Huo, Q. Li, Y. Zhang, C. Hou and Y. Lei, *Sensor Actuat B: Chem*, 2014, **199**, 410-417.
6. Z. H. Ibupoto, K. Khun, V. Beni, X. Liu and M. Willander, *Sensors*, 2013, **13**, 7926-7938.
7. L. Changli, Y. Hiroyasu, L. Yaerim, T. Hitoshi and D. Jean-Jacques, *Acs Sym Ser*, 2015, **26**, 305503.
8. Í. A. Simon, N. G. Medeiros, K. C. Garcia, R. M. D. Soares, A. T. Rosa and J. A. Silva, *Journal of the Brazilian Chemical Society*, 2015, **26**, 1710-1717.
9. R. Ahmad, N. Tripathy, Y.-B. Hahn, A. Umar, A. A. Ibrahim and S. H. Kim, *Dalton Transactions*, 2015, **44**, 12488-12492.
10. A.-m. Cao, J. D. Monnell, C. Matranga, J.-m. Wu, L.-l. Cao and D. Gao, *J. Phys. Chem C*, 2007, **111**, 18624-18628.
11. V. Senthilkumar, Y. S. Kim, S. Chandrasekaran, B. Rajagopalan, E. J. Kim and J. S. Chung, *RSC Adv*, 2015, **5**, 20545-20553.
12. Z. H. Ibupoto, A. Nafady, R. A. Soomro, Sirajuddin, S. T. Hussain Sherazi, M. I. Abro and M. Willander, *RSC Adv*, 2015, **5**, 18773-18781.
13. Y. T. Liu, J. Deng, X. L. Xiao, L. Ding, Y. L. Yuan, H. Li, X. T. Li, X. N. Yan and L. L. Wang, *Electrochim. Acta*, 2011, **56**, 4595-4602.
14. A. Kamran and S. Rizvi, in *Proceedings of the Sixth International Conference on Management Science and Engineering Management*, eds. J. Xu, M. Yasinzai and B. Lev, Springer London, 2013, vol. 185, ch. 79, pp. 909-924.
15. H. Miao, S. Fan, Y. N. Wu, L. Zhang, P. P. Zhou, J. G. Li, H. J. Chen and Y. F. Zhao, *Biomedical and environmental sciences : BES*, 2009, **22**, 87-94.
16. G. Venkatasami and J. R. Sowa Jr, *Anal. Chim. Acta*, 2010, **665**, 227-230.
17. J. Cheng and X. O. Su, *Guang pu xue yu guang pu fen xi = Guang pu*, 2011, **31**, 131-135.
18. H. A. Cook, C. W. Klampfl and W. Buchberger, *Electrophoresis*, 2005, **26**, 1576-1583.
19. Q. Cao, H. Zhao, Y. He, N. Ding and J. Wang, *Anal Chim Acta*, 2010, **675**, 24-28.
20. C.-W. Liao, Y.-R. Chen, J.-L. Chang and J.-M. Zen, *Electroanalysis*, 2011, **23**, 573-576.

21. H. Akter, A. A. Shaikh, T. R. Chowdhury, M. S. Rahman, P. K. Bakshi and A. J. S. Ahammad, *ECS Electrochemistry Letters*, 2013, **2**, B13-B15.
22. K. Rovina and S. Siddiquee, *Food Control*, 2016, **59**, 801-808.
23. C.-W. Liao, Y.-R. Chen, J.-L. Chang and J.-M. Zen, *Journal of Agricultural and Food Chemistry*, 2011, **59**, 9782-9787.
24. P. Taheri, J. Wielant, T. Hauffman, J. R. Flores, F. Hannour, J. H. W. de Wit, J. M. C. Mol and H. Terryn, *Electrochim. Acta*, 2011, **56**, 1904-1911.
25. M. A. Dar, Q. Ahsanulhaq, Y. S. Kim, J. M. Sohn, W. B. Kim and H. S. Shin, *Appl. Surf. Sci*, 2009, **255**, 6279-6284.
26. Q. Cao, H. Zhao, L. Zeng, J. Wang, R. Wang, X. Qiu and Y. He, *Talanta*, 2009, **80**, 484-488.

Figure Captions

Figure.1 The FEG-SEM captures of marigold-like nanostructures at different magnifications reflecting sharp and populated structural features

Figure 2 The recorded XRD pattern for marigold like CuO nanostructures

Figure 3 The XPS spectra of mari-gold like CuO nanostructures with inset regional scan of Cu 2p and O1s binding energies

Figure 4 The electrochemical evaluation of (a) GCE/CuO-NSs/nafion (b) CuO (template free) in presence of 0.1 μM melamine 0.1 M (pH 6.5) PBS buffer

Figure 5. CV measurement of GCE/CuO-NSs/nafion (a) at scan rates from 0.05-0.11Vs^{-1} with inset figure depicting linearity of redox response against square root of scan rate (b) at different pH in range from 7-9 (c) at various deposition volume of as-synthesised CuO nanostructures suspension in range from 5-20μL with inset graph reflecting the unstable response measured for 20μL of deposition volume

Figure 6. SWV measurements of GCE/CuO-NSs/nafion for melamine in concentration range from 0.1 to 5.6×10^{-9} M (b) the corresponding calibration plot with linear fit regression

Figure 7. The evaluation of GCE/CuO-NSs/nafion for (a) selectivity in presence of common interferents (b) reproducibility during number of measurements (c) stability during the storage period of six weeks in ambient air atmosphere

Table 1 Comparison of developed electrochemical sensor with various recent reported protocols for determination of melamine

Methods	LOD	Linear Range	Recovery (%)	Reference
Electrochemical				
Oligonucleotides modified gold electrode	3.0×10^{-9} M	1.0×10^{-8}–5.0×10^{-6} M	96	[26]
Electrochemical Accumulation Coupled with Enzyme	0.36 µM	4.0 µM–0.45 mM	95.6–105.2	[27]
Gold NPS-Modified Indium Tin Oxide Electrode	0.13 ppb	5–500 $\times10^{-9}$ M	99.2–100.8	[28]
GCE/CuO-NSs/nafion	**0.1×10^{-10} M**	**0.1×10^{-9}– 5.6×10^{-9} M**	**98–99**	**This work**
Fourier Transform Infrared Spectroscopy (FTIR)				
SB-ATR	2.5 ppm	25–0.0625 %	95.44– 102.0	[29]
FTIR	1 ppm	0.001–1 %	98.9–100.2%	[30]
Chromatographic Methods				
ICEMS	0.01mg kg^{-1}	0.5–100 ng mL^{-1}	86–89%	[31]
GC-UPLC-MS	10 and 5 g kg^{-1}	1–1000µ gL^{-1} 5–1000µ gL^{-1}	85.2–103.2%	[32]

Table 2 Melamine determination from milk and urine samples

Sample Type	***Added (M)***	***Found(M) mean*± standard deviation***	***Recovery (%)***	***RSD (%)***
Milk				
1	2.0×10^{-9}	$1.98\times10^{-9}\pm 1.2\times10^{-9}$	99	0.52
2	2.0×10^{-9}	$1.96\times10^{-9}\pm 1.3\times10^{-9}$	98	0.75
3	2.0×10^{-9}	$1.97\times10^{-9}\pm 0.9\times10^{-9}$	98.5	0.31
4	2.0×10^{-9}	$1.98\times10^{-9}\pm 1.0\times10^{-9}$	99	0.83
Urine				
1	2.0×10^{-9}	$1.95\times10^{-9}\pm 1.4\times10^{-9}$	97.5	0.83
2	2.0×10^{-9}	$1.99\times10^{-9}\pm 1.0\times10^{-9}$	99.5	0.62
3	2.0×10^{-9}	$1.94\times10^{-9}\pm 1.3\times10^{-9}$	97	0.51
4	2.0×10^{-9}	$1.97\times10^{-9}\pm 1.2\times10^{-9}$	98.5	0.58

***** Three repetitive measurements

Figure.1

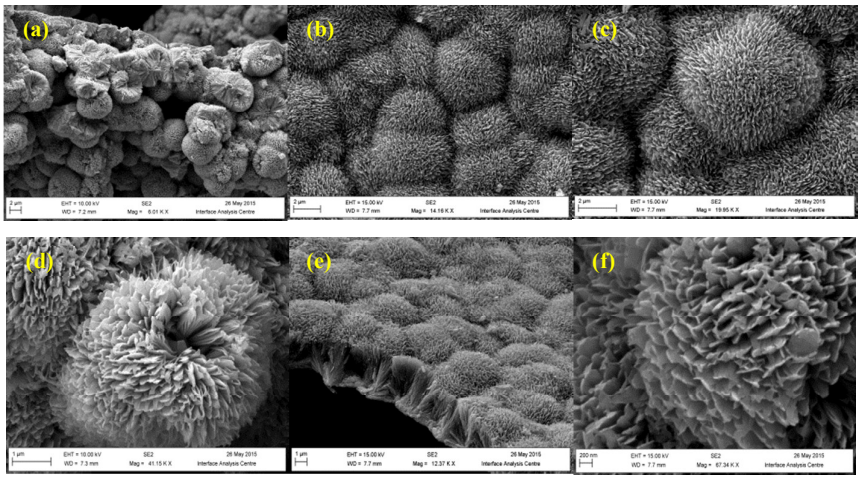

Figure 2

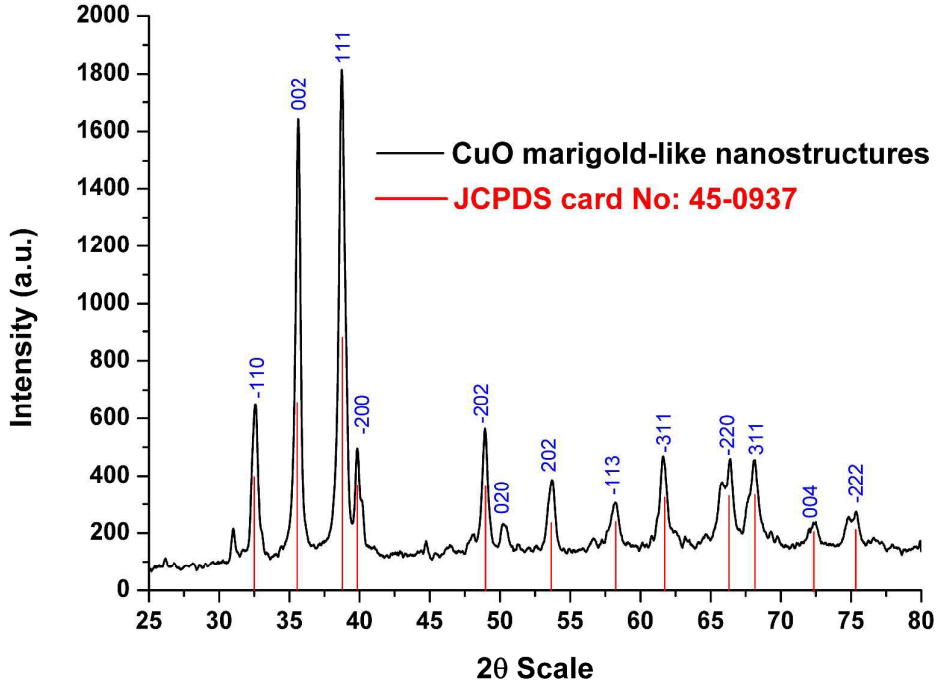

Figure 3

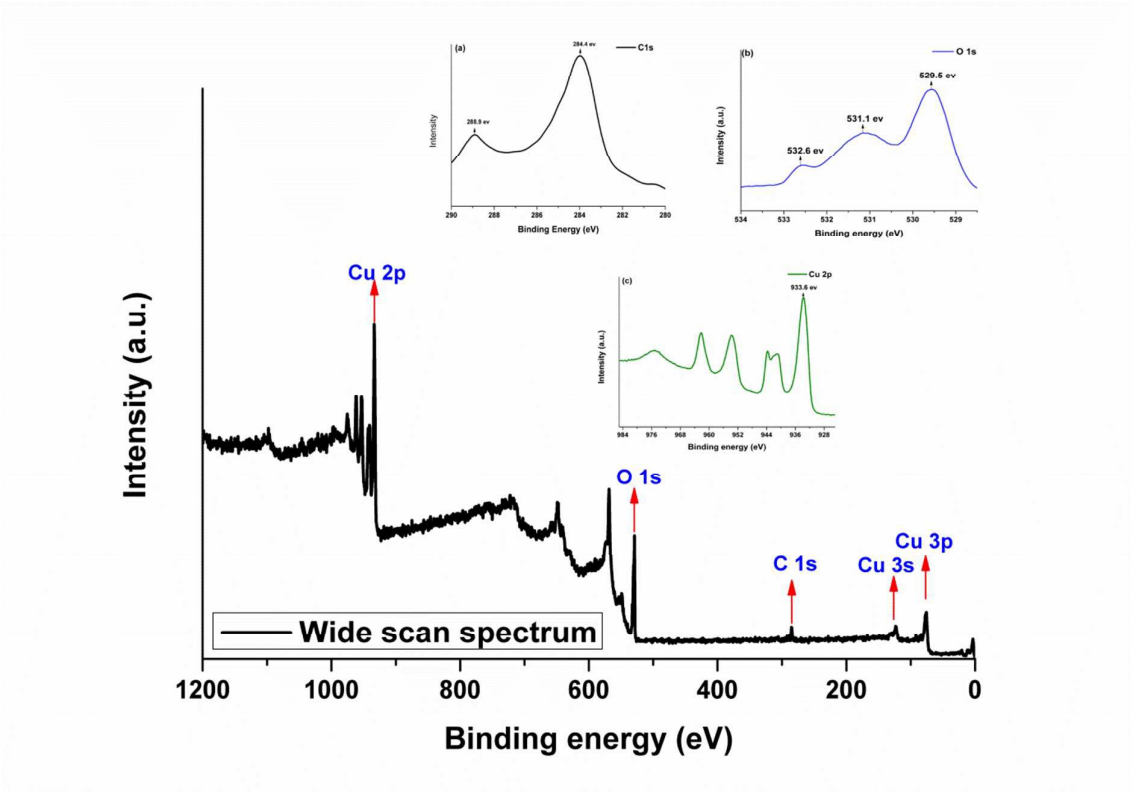

Figure 4

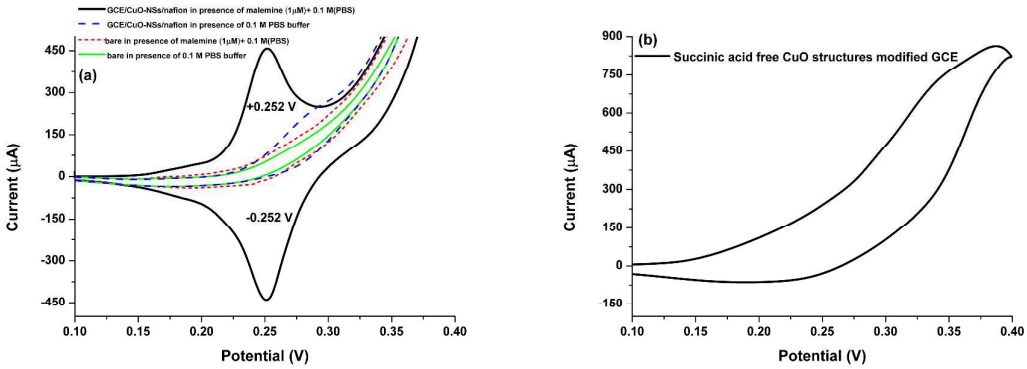

Figure 5

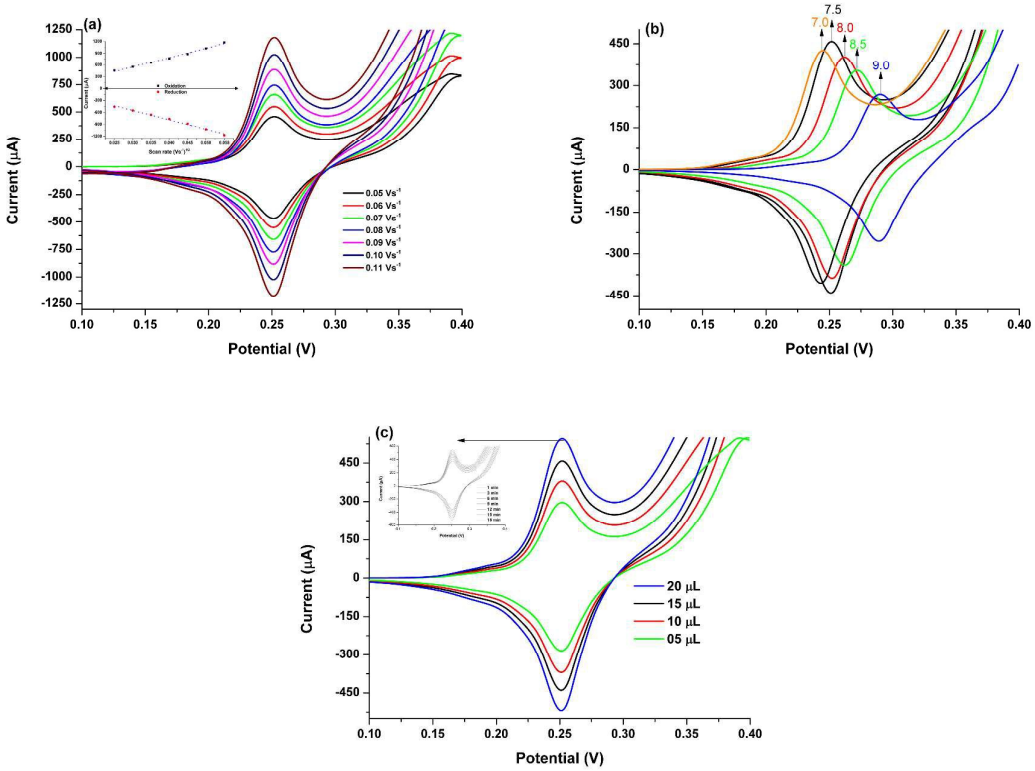

Figure 6

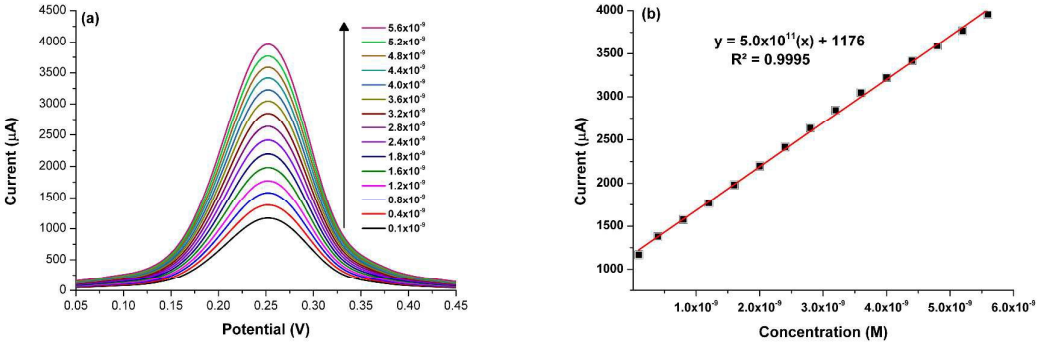

Figure 7